American Society of Hematology
2021 L Street NW, Suite 900,
Washington, DC 20036
Phone: 202-776-0544 | Fax 202-776-0545
editorial@hematology.org

BET-bromodomain and EZH2 inhibitor treated chronic GVHD mice have blunted germinal centers with distinct transcriptomes

Tracking no: BLD-2021-014557R1

Michael Zaiken (University of Minnesota, United States) Ryan Flynn (University of Minnesota, United States) Katelyn Paz (University of Minnesota, United States) Stephanie Rhee (University of Minnesota, United States) Sujeong Jin (University of Minnesota, United States) Fathima Mohamed (University of Minnesota, United States) Asim Saha (University of Minnesota, United States) Govindarajan Thangavelu (University of Minnesota, United States) Paul Park (Dana-Farber Cancer Institute, United States) Matthew Hemming (Dana-Farber Cancer institute, United States) Peter Sage (Brigham and Women's Hospital, United States) Arlene Sharpe (Harvard Medical School and Brigham and Women's Hospital, United States) Michel DuPage (Massachusetts Institute of Technology, United States) Jeffrey Bluestone (University of California, San Francisco, United States) Angela Panoskaltsis-Mortari (University of Minnesota, United States) Corey Cutler (Dana Farber Cancer Institute, United States) John Koreth (Dana-Farber Cancer Institute, United States) Joseph Antin (Dana-Farber Cancer Institute, United States) Robert Soiffer (Dana-Farber Cancer Institute, United States) Jerome Ritz (Dana-Farber Cancer Institute; Harvard Medical School, United States) Leo Luznik (Sidney Kimmel Cancer Center, United States) Ivan Maillard (University of Pennsylvania, United States) Geoffrey Hill (Fred Hutchinson Cancer Research Center, United States) Kelli MacDonald (Queensland Institute of Medical Research, Australia) David Munn (Augusta University, United States) Jonathan Serody (University of North Carolina, Lineberger Comprehensive Cancer Center, United States) William Murphy (University of California, Davis, United States) Leslie Kean (Dana-Farber/Boston Children's Cancer and Blood Disorders Center, United States) Yi Zhang (Fels Institute for Cancer Research and Molecular Biology, Temple University, United States) James Bradner (Dana-Farber Cancer Institute, United States) Jun Qi (Dana-Farber Cancer Institute, United States) Bruce Blazar (University of Minnesota, United States)

Abstract:
Despite advances in the field, chronic graft-vs-host-disease (cGVHD) remains a leading cause of morbidity and mortality following allogenic hematopoietic stem cell transplant. As treatment options remain limited, we tested efficacy of anti-cancer, chromatin modifying enzyme inhibitors in a clinically relevant murine model of cGVHD with bronchiolitis obliterans (BO). We observed that the novel Enhancer of Zeste Homolog 2 (EZH2) inhibitor JQ5, and the BET-bromodomain inhibitor JQ1 each improved pulmonary function, impaired the germinal center (GC) reaction, a prerequisite in cGVHD/BO pathogenesis, and JQ5 reduced EZH2-mediated H3K27me3 in donor T cells. Using conditional EZH2 knockout donor cells we demonstrated that EZH2 is obligatory for the initiation of cGVHD/BO. In a sclerodermatous cGVHD model, JQ5 reduced the severity of cutaneous lesions. To determine how the two drugs could lead to the same physiological improvements while targeting unique epigenetic processes we analyzed the transcriptomes of splenic GCB cells (GCBs) from transplanted mice treated with either drug. Multiple inflammatory and signaling pathways enriched in cGVHD/BO GCBs were reduced by each drug. GCBs from JQ5 but not JQ1 treated mice were enriched for pro-proliferative pathways also seen in GCBs from BM-Only transplanted mice, likely reflecting their underlying biology in the unperturbed state. In conjunction with *in vivo* data these insights lead us to conclude that epigenetic targeting of the GC is a viable clinical approach for the treatment of cGVHD, and that the EZH2 inhibitor JQ5 and the BET-bromodomain inhibitor JQ1 demonstrated clinical potential for EZH2i and BETi in patients with cGVHD/BO.

Conflict of interest: COI declared - see note

COI notes: BRB receives remuneration as an advisor to Magenta Therapeutics and BlueRock Therapeutics; Research funding from BlueRock Therapeutics, Rheos Medicines, Equilibre biopharmaceuticals, Carisma Therapeutics, Inc., and is a co-founder of Tmunity Therapeutics. JQ is a scientific co-founder and consultant for Epiphanes; and consultant for Talus. GRH has consulted for Generon Corporation, NapaJen Pharma, iTeos Therapeutics, Neoleukin Therapeutics and has received research funding from Compass Therapeutics, Syndax Pharmaceuticals, Applied Molecular Transport, Serplus Technology, Heat Biologics, Laevoroc Oncology and iTeos Therapeutics.

Preprint server: No;

Author contributions and disclosures: M.Z. designed experiments, performed experiments, and wrote the paper. R.F. Designed and performed experiments. K.P., S.R., S.J., F.M., S.A., and G.T., performed and assisted with experiments. P.M.P., M.L.H., P.T.S., L.S.K. assisted with bioinformatic analyses. J.Q., J.E.B., synthesized and provided reagents and discussed experiments. J.A.B. and M. DuPage provided mice for experiments. A.H.S., C.S.C., J.K, J.H.A., R.J.S., J.R., L.L., I.M., G.R.H, K.P.M, D.H.M., J.S.S, W.J.M., Y.Z. discussed experiments, results and conclusions. J. Q., B.R.B designed experiments, reviewed data, and assisted in manuscript preparation. All authors edited the manuscript.

Non-author contributions and disclosures: No;

Agreement to Share Publication-Related Data and Data Sharing Statement: PRJNA773813

Clinical trial registration information (if any):

BET-bromodomain and EZH2 inhibitor treated chronic GVHD mice have a blunted germinal centers with distinct transcriptomes

Zaiken M[1], Flynn R[1], Paz K[1], Rhee S[1], Jin S[1], Mohamed F[1], Saha A[1], Thangavelu G[1], Park PM[2], Hemming ML[2], Sage PT[3], Sharpe AH[3], DuPage M[4,5], Bluestone JA[6], Panoskaltsis-Mortari A[1], Cutler CS[7], Koreth J[7], Antin JH[7], Soiffer RJ[8], Ritz J[7], Luznik L[9], Maillard I[10], Hill GR[11,12], MacDonald KP[13], Munn DH[14], Serody JS[15], Murphy WJ[16], Kean LS[2], Zhang Y[18], Bradner JE[19,20], Qi J[2,21], Blazar BR[1]

1) Division of Blood & Marrow Transplant & Cellular Therapy, Department of Pediatrics, Masonic Cancer Center, University of Minnesota, Minneapolis, Minnesota.
2) Department of Cancer Biology, Dana-Farber Cancer Institute, Boston, MA 02215, USA
3) Department of Immunology, Blavatnik Institute, Harvard Medical School, Boston, MA 02115, USA; Evergrande Center for Immunologic Diseases, Harvard Medical School and Brigham and Women's Hospital, Boston, MA 02115, USA.
4) David H. Koch Institute for Integrative Cancer Research, Massachusetts Institute of Technology, Cambridge, MA, USA.
5) Division of Immunology and Pathogenesis, Department of Molecular and Cell Biology, University of California Berkeley, Berkeley, CA, USA.
6) University of California San Francisco, San Francisco, CA, USA
7) Division of Hematologic Malignancies, Dana-Farber Cancer Institute, Harvard Medical School, Boston, Massachusetts.
8) Department of Medical Oncology, Dana-Farber Cancer Institute, Harvard Medical School, Boston, MA 02215, USA
9) Department of Oncology, Sidney Kimmel Cancer Center, Baltimore, Maryland
10) Division of Hematology-Oncology, Department of Medicine, University of Pennsylvania, Philadelphia, PA.
11) Clinical Research Division, Fred Hutchinson Cancer Research Center, Seattle, WA.
12) Division of Medical Oncology, University of Washington, Seattle, WA.
13) Department of Immunology, Queensland Institute of Medical Research (QIMR), University of Queensland, Brisbane, QLD, Australia.
14) Georgia Cancer Center, Augusta University, Augusta, GA.
15) Lineberger Comprehensive Cancer Center, University of North Carolina, Chapel Hill, NC.
16) Department of Dermatology, School of Medicine, University of California, Davis, Sacramento, CA.
17) Boston Children's Hospital, Dana-Farber Cancer Institute, Boston, MA
18) Fels Institute for Cancer Research and Molecular Biology; Department of Microbiology and Immunology, Temple University, Philadelphia, PA.
19) Department of Medical Oncology, Dana-Farber Cancer Institute, Boston, MA
20) Current affiliation: Novartis Institute of Biomedical Research, Cambridge, MA
21) Department of Medicine, Harvard Medical School, Boston, MA

Corresponding Author Information:

Bruce R Blazar; MMC 366, University of Minnesota, 420 Delaware St SE, Minneapolis, MN 55455; Email: blaza001@umn.edu; Phone: 612-626-2734

Jun Qi; Department of Cancer Biology, Dana-Farber Cancer Institute, Boston; Email: jun_qi@dfci.harvard.edu.

Abstract Word Count: 247/250

Text Word Count: 3976/4000

Figure Count: 6 + 3 supplementary figures

Reference Count: 81

Key Points:

- Novel EZH2 inhibitor JQ5 and BET-Bromodomain inhibitor JQ1 reduce pulmonary dysfunction and blunt germinal center response in murine cGVHD
- Despite similar physiological impacts, JQ1 and JQ5 induce distinct transcriptional changes that independently disrupt the germinal center.

Abstract:

Despite advances in the field, chronic graft-vs-host-disease (cGVHD) remains a leading cause of morbidity and mortality following allogenic hematopoietic stem cell transplant. As treatment options remain limited, we tested efficacy of anti-cancer, chromatin modifying enzyme inhibitors in a clinically relevant murine model of cGVHD with bronchiolitis obliterans (BO). We observed that the novel Enhancer of Zeste Homolog 2 (EZH2) inhibitor JQ5, and the BET-bromodomain inhibitor JQ1 each improved pulmonary function, impaired the germinal center (GC) reaction, a prerequisite in cGVHD/BO pathogenesis, and JQ5 reduced EZH2-mediated H3K27me3 in donor T cells. Using conditional EZH2 knockout donor cells we demonstrated that EZH2 is obligatory for the initiation of cGVHD/BO. In a sclerodermatous cGVHD model, JQ5 reduced the severity of cutaneous lesions. To determine how the two drugs could lead to the same physiological improvements while targeting unique epigenetic processes we analyzed the transcriptomes of splenic GCB cells (GCBs) from transplanted mice treated with either drug. Multiple inflammatory and signaling pathways enriched in cGVHD/BO GCBs were reduced by each drug. GCBs from JQ5 but not JQ1 treated mice were enriched for pro-proliferative pathways also seen in GCBs from BM-Only transplanted mice, likely reflecting their underlying biology in the unperturbed state. In conjunction with *in vivo* data these insights lead us to conclude that epigenetic targeting of the GC is a viable clinical approach for the treatment of cGVHD, and that the EZH2 inhibitor JQ5 and the BET-bromodomain inhibitor JQ1 demonstrated clinical potential for EZH2i and BETi in patients with cGVHD/BO.

Introduction

Chronic graft-vs-host disease (cGVHD) is a life-threatening, multi-organ, autoimmune like condition that arises late following allogeneic hematopoietic stem cell transplantation (alloHSCT). Despite recent advances, cGVHD remains the leading cause of morbidity and non-relapse associated mortality following alloHSCT, arising in 30-70% of patients.[1–6] Treatment options remain limited. First-line treatment involves corticosteroids resulting in a 50-60% response rate, more global immunosuppression and potential serious side effects.[7] There has been increasing emphasis on more immunomodulatory and less immunosuppressive pharmacologic agents. Ibrutinib, a Bruton's tyrosine kinase (BTK) and IL2-inducible kinase (ITK) inhibitor, was the first approved therapy for steroid-refractory cGVHD patients failing systemic therapies.[5,6] Belumosudil (KD025; REZUROCK), a Rho-associated coiled-coil kinase 2 (ROCK2) inhibitor, was approved for cGVHD patients failing two or more lines of systemic therapy.[8] In a randomized phase III trial, ruxolitinib (Jakifi), a Janus activated kinase (JAK)1/2 inhibitor, showed superiority for treating steroid-refractory or steroid-dependent cGVHD patients failing <2 prior systemic therapies most recently received FDA approval.[9] Complete responses were infrequent and drug associated side-effects (e.g. cytopenia's; infections) were observed, demonstrating a clear medical need for additional therapies.

Of the cGVHD manifestations, sclerodermatous and pulmonary cGVHD remain treatment challenges.[10,11] Well-established preclinical murine scleroderma models have been used as a platform for testing new agents.[12,13] A murine multiorgan system cGVHD model with bronchiolitis obliterans (BO) was developed that is germinal center (GC) formation-dependent. The production and lung deposition of allo- and/or auto- antibodies, monocyte and macrophage recruitment and activation results in pro-fibrogenic molecule release, fibroblast secretion of

extra-cellular matrix including collagen and fibrosis, suggesting that modulation or inhibition of the GC reaction may be a new therapeutic target..[14–16]

Enhancer of Zeste Homolog 2 (EZH2), a histone-lysine N-methyltransferase and the catalytic component of the Polycomb Repressive Complex 2 (PCR2), is a critical regulator in GC formation and proliferation/differentiation of antibody secreting B cells.[17,18] EZH2 catalyzes the trimethylation of lysine 27 on histone 3 (H3K27me3), impairing target gene transcription, and has a key role in establishing bivalent chromatin domains that regulate cell fate determination. [19–24] EZH2 overexpression is seen in a diffuse array of tumors, including B cell and T cell malignancies[25], and associated with a poor prognosis.[26,27] Of available EZH2 inhibitors, we tested a readily translatable, high potency, and bioavailable compound, JQEZ5 (JQ5), for effects in sclerodermatous and cGVHD/BO models.[28]

Other GC targeting were directed to bromodomain and extra terminal (BET) enzymes. Bromodomains (BRD) recognize histone acetylated lysine motifs and initiate transcriptional activation to drive gene expression. Small molecule inhibitors competitively bind BRD preventing histone acetylated lysine engagement, decreasing expression of genes involved in cell proliferation, differentiation, and cytokine/chemokine production.[29] For example, *in vitro* the BET inhibitor JQ1 hinders T cell IL21 expression required for T follicular helper cell (TFH) function.[30] *In vivo* JQ1 impaired GC B cell (GCB) formation via BCL6 repression in 4-Hydroxy-3-nitrophenyl-chicken gamma globulin (NP-CGG) immunized mice.[31] In culture and murine systemic lupus erythematosus models, cytokines, B-cell activating factor (BAFF) and IL17, implicated in cGVHD pathology, were suppressed. In a murine acute GVHD (aGVHD) model, the selective pan-BET inhibitor, I-BET151, reduced inflammatory cytokines, improving survival

and pathology.[32] These properties pointed to JQ1 therapeutic potential for sclerodermatous and pulmonary cGVHD.

Since both EZH2 and BRD4 are upregulated in GCBs, we hypothesized JQ1 and JQ5 would effectively treat murine cGVHD/BO. In testing this, we investigated JQ5 and JQ1 as novel treatments for cGVHD, established EZH2 necessity in both the BM and T cell graft compartments for cGVHD/BO initiation, and identified that JQ5 has therapeutic potential in both BO and sclerodermatous cGVHD models whereas JQ1 only mitigated disease in a cGVHD/BO model. By comparing GCB transcriptomes from mice with cGVHD/BO treated with each compound we offer potential mechanistic explanations for these observations. Given the recent FDA approval of EZH2 inhibitors and more than a dozen BRD inhibitors in clinical trials, our study helps establish the preclinical rationale on both targets for cGVHD treatment.

Materials and Methods

Mice

C57Bl/6 (B6) ($H2^b$) mice were purchased from the National Cancer Institute through Charles River Laboratories. B10.BR ($H2^k$), BALB/c ($H2^d$), and B10.D2 ($H2^d$) mice were purchased from Jackson Laboratories. EZH2 fl/fl provided by Drs. Michel DuPage and Jeffrey Bluestone were bred to CD4-Cre and CD19-Cre mice at the University of Minnesota animal facility.[33,34] All mice were housed in a specific pathogen-free facility and used with University of Minnesota institutional animal care and use committee approval.

Bone Marrow Transplant (BMT)

In the cGVHD/BO model, B10.BR recipients were conditioned with 120mg/kg Cytoxan (days -3,-2) and 7.6 Gy total body irradiation (TBI) (day-1). Donor (B6) BM was T cell depleted with anti-CD4/anti-CD8 monoclonal antibodies and rabbit complement. Splenic T cells were purified using anti-CD19 (eBio:13-0193-85), anti-B220 (Stemcell Tech:60019BT), anti-CD11b (Stemcell Tech:60001BT), anti-CD11c (Stemcell Tech:60002BT), anti-TCRγ/δ (BD:553176), anti-NK1.1 (eBio:13-5941-85), and anti-TER119 (eBio:13-5921-85) antibodies and magnetic beads (Stemcell:50001). Recipients received $10x10^6$ purified BM cells ± $73.5x10^3$ B6 purified T cells. Mice were monitored daily for survival, clinical and skin scores twice weekly, and weights recorded weekly.[14,16] In the sclerodermatous model, B10.D2 BM ($10x10^6$) and T cells ($2.7x10^6$; 2:1 CD4:CD8 ratio) were given to BALB/c recipients after 7.0 Gy TBI (day -1).[35] Mice were monitored daily and assessed for clinical score and skin score as described.[36]

JQ1 and JQ5 preparation and administration

JQ5 and JQ1 were provided by Drs. Jay Bradner and Jun Qi.[28,37] Both compounds were characterized using NMR, HRMS, and HPLC to confirm the identity and purity. JQ5 was synthesized and purified by flash chromatography and prep-HPLC.[37] JQ1 was synthesized to produce racemic JQ1, as published.[28] cGVHD mice were injected intraperitoneally with JQ5 (75mg/kg) or JQ1 (50mg/kg) in 10% 2-Hydroxypropyl)-β-cyclodextrin (HPbCD) or vehicle thrice weekly from day 28 (cGVHD/BO onset) until day 49.

Pulmonary Function Tests

Mice were anesthetized and ventilated using the Flexivent system (Scireq). Pulmonary resistance, elastance, and compliance were measured using Flexivent Software v5.1. [14]

Frozen Tissue Preparation

At time of sacrifice, lungs were intratracheally inflated with 75% Tissue-Tek optimal cutting temperature compound (OCT) (Cat. # 4583). Tissue blocks were flash frozen and stored at -80C.

Immunofluorescence (IF)

For IF assays, 8-um cryostections were cut and acetone fixed. For immunoglobulin (Ig) deposition experiments, lung sections were stained with goat anti-mouse FITC conjugated antibody (BD:553585), and DAPI (4′,6-diamidino-2-phenylindole) containing mounting medium (Vector Labs:H-2000-10). For GC detection, spleen sections were stained with rhodamine-peanut agglutinin (Vector Labs:RL-1072), anti-CD4 FITC (ThermoFisher:11-0042-82) antibody and mounted in DAPI mounting medium (Vector Labs:H-2000-10). Images were taken on an EVOS microscope. Analysis was performed using EBImage via calculation of the percentage of pixels most positive in the FITC channel vs those in the DAPI channel.[38] Voronoi tessellation was used to identify the central peanut agglutinin (PNA)+ region of the images, and quantified as percent total pixels in the image.

Frozen Tissue Preparation, Histology and Histochemistry

Sections 8-μM cryosections were either fixed overnight at room temperature in Bouin's solution (Sigma:HT10132-1L) and stained using Masson's trichrome staining kit (Sigma:HT15-1KT) or stained with hematoxylin (Sigma:GHS332) and eosin (Sigma:HT110116) for pathology. Histopathology scoring on coded sections was performed as previously described by a double-blinded researcher.[39] Trichrome images were analyzed using EBImage.[38]

Flow Cytometry

Flow cytometry of organ suspensions was performed on day 49 post-BMT. For GC cells, spleens were stained with fixable-viability dye (ThermoFisher:65-0865-14), anti-CD4 (BD:563726), anti-CXCR5 (eBio:12-7185-82), anti-PD1 (ThermoFisher:63-9981-82), anti-CD19 (ThermoFisher:61-0193-82), anti-GL7 (eBio:45-5902-82), and anti-FAS (BD:563646). Suspensions were fixed and permeabilized using FoxP3 transcription factor staining kit (eBio:00-5523-00), intracellularly stained with anti-FoxP3 (eBio:25-5773-82) and in some studies anti-H3K27me3 (Abcam:ab205728). For plasma cell (PC) analysis, lung suspensions were stained with fixable-viability dye (ThermoFisher:65-0865-14), anti-CD38 (BioLegend:102718), anti-CD19 (ThermoFisher:61-0193-82), and anti-B220 (BD:562922). Samples were analyzed on a BD LSRFortessaII.

RNAseq Sample Preparation

Day 49 post-BMT spleens were homogenized, RBC lysed, stained for FACS sorting with fixable-viability dye, anti-CD19, anti-GL7, and anti-FAS (same products as above) and ≥100,000 cells were collected directly into an equivalent volume of Qiagen buffer RLT (Qiagen:74134) + 1% 2-ME (Sigma:M6250-100ML). Samples were frozen on dry ice until processing at University of Minnesota Genomics Center. RNA was collected and isolates quantified by fluorometric RiboGreen assay, integrity determined using capillary electrophoresis and samples converted to sequencing libraries using Takara Bio's SMARTer Stranded Total RNA-Seq–Pico Mammalian Kit v2 (634414).

RNAseq Analysis

Indexed libraries were normalized, pooled, and loaded onto a NovaSeq paired end flow cell for clustering and sequencing using Illumina's bcl2fastq v2.20. FASTQ reads were entered into the Collection of Hierarchical UMII/RIS Pipelines[40] for quality control[41], trimming, confirming viability, aligning reads[42] using HISAT2[43], filtering alignments using SAMtools[44] and generating output matrices using Subread FeatureCounts[45]. Genome alignments were run against the mm10 reference genome (GRCm38). Resulting counts were analyzed for differential gene expression using DEseq2.[46]

Data Sharing

Data can be found at accession number PRJNA773813.

Results

Epigenetic modifying enzyme inhibitors to BET bromodomains or EZH2 effectively treated murine cGVHD/BO

Considering epigenetic modifying enzyme inhibitor effects on GC reactions, we investigated the BET-bromodomain inhibitor JQ1 and the novel EZH2 inhibitor JQ5 in a multi-organ cGVHD/BO model. We tested a novel EZH2 inhibitor as other commonly tested EZH2 inhibitors were ineffective in our model. UNC1999 showed toxicity (<50% survival over treatment period) (Supplementary Figure 1A), while DZnep had no impact on the pulmonary function of treated mice (Supplementary Figure 1B).[47,48]

B10.BR mice were conditioned with Cytoxan and TBI, transplanted with B6 donor BM ± a low supplemental T cell dose ($73.5x10^3$). Chronic GVHD mice were treated with JQ5 (75mgkg

JQ5), JQ1 (50mg/kg) or vehicle IP from days 28-49. Both JQ5 (Figure 1A) and JQ1 (Figure 1B) significantly ($p<0.01$) improved day 49 pulmonary function across all parameters, though without significant impacts on weights or overall survival of treated mice, which is not unexpected as both weight loss and mortality are limited in this model (Supplementary Figure 2).[49] The use of whole body plethysmography to assess disease progression provides a clinically relevant functional measure of pulmonary function, above and beyond simple measures like respiratory rate, as these tests are directly analogous to the pulmonary function testing done in a clinical setting to diagnose, track, and manage bronchiolitis obliterans.[50] To determine whether improvements were associated with decreased pulmonary fibrosis, lung cryosections were stained for collagen and Ig deposition. Pulmonary sections showed a significant ($p<0.001$) reduction in collagen deposition in JQ5 (Figure 1C) or JQ1 (Figure 1D) treated mice compared to vehicle controls. Lung IF staining for Ig deposition showed a near complete absence of IgG of JQ5 (Figure 1E) and JQ1 (Figure 1F) treated mice. Hematoxylin and Eosin staining of other target organs including the large intestine, liver, and spleen showed reduced histology scores with both JQ5 and JQ1 treatment, albeit only statistically significantly in lungs (Supplementary Figure 3). Together our studies show JQ5 and JQ1 each reduced murine cGVHD/BO severity.

JQ5 and JQ1 impaired the murine cGVHD/BO GC reaction

Since BRD4 and EZH2 are upregulated in GCBs and GCs are critical for cGVHD/BO pathogenesis, we assessed whether the observed reduction in pulmonary severity was accompanied by a GC response reduction.[16,18] For both drugs the GC reaction was significantly ($p<0.05$) inhibited, evidenced by decreased splenic TFH and GCB frequency and increased splenic T follicular regulatory cell (TFR) frequency and TFR/TFH ratio (Figures 2A—2C).

Spleen cryosections were stained with rhodamine-PNA, anti-CD4 FITC, and DAPI and images were analyzed for GC numbers per unit area in each spleen section and average size (Figure 2D). JQ5 (Figure 2E) and JQ1 (Figure 2F) showed a significantly ($p<0.05$) lower GC number per mm^2 and average GC size.

To determine if the reduced GC response decreased pulmonary plasma cell (PC) frequency of drug-treated cGVHD/BO mice, PC (CD138+ lymphocytes), immature PC (CD19+, B220+) and mature PC (CD19-, B220-) frequencies were quantified. While total lung resident PCs were largely unchanged between conditions, a significant ($p<0.05$) reduction in frequency of the mature, antibody-secreting, CD19- B220- PC subpopulation was observed (Figure 2G). EZH2 inhibition by JQ5 was predicted to decrease in H3K27me3 in GC cells. Therefore, total H3K27me3 present in GC populations was quantified. JQ5 vs vehicle treated mice had significantly reduced H3K27me3 in TFH, TFR and GCB cells (Figures 2H and 2I).

EZH2 expression is necessary in donor BM and T cells for murine cGVHD/BO and GC responses

Since EZH2 is upregulated in T cells and B cells in GCs that play a significant role in cGVHD pathogenesis,[15,16,36,51] EZH2 was selectively deleted in donor T cells that give rise to TFHs or BM B cells that produce GCBs. B10.BR recipients were transplanted with wildtype (WT) B6 or EZH2 knockout (ko) BM from EZH2 fl/fl CD19 Cre donors ± purified WT B6 T cells. On day 49 we observed significant ($p<0.05$) improvement in pulmonary function in recipients of EZH2 fl/fl CD19 Cre vs WT BM (Figure 3A). To assess EZH2 effects in donor T cells, mice were given WT B6 BM + WT or EZH2 fl/fl CD4 Cre T cells. Mice receiving EZH2 ko T cells showed significant ($p<0.01$) improvement in pulmonary function (Figure 3B).

Recipients of EZH2 ko T cells or EZH2 ko BM cells had a significant reduction in lung collagen (Figures 3C and 3F) and IgG deposition (Figure 3D and 3E).

Next, we sought to determine if EZH2 expression was required in GCBs to mediate murine cGVHD/BO. Mice transplanted with B6 donor EZH2 fl/fl CD19 Cre BM + WT T cells had a significant ($p<0.05$) reduction TFHs and GCBs along with an increase in TFR and TFR/TFH ratio, implicating EZH2 expression in GCBs as a key regulator of the GC response (Figure 4A). Mice transplanted with B6 donor WT BM + EZH2 fl/fl x CD4-Cre T cells had a significant ($p<0.05$) reduction TFHs and GCBs and an increased TFR/TFH ratio. Tissue analyses paralleled immune analyses (Figure 4). Recipients of WT BM + EZH2 fl/fl x CD4-Cre vs WT T cells had significantly reduced GC numbers and size (Figure 4D). GC size also was reduced in recipients of EZH2 fl/fl x CD19-Cre vs WT BM + WT T cells. Together, these findings demonstrate that donor TFH and GCB cell EZH2 expression in donor TFHs and GCBs is essential for cGVHD/BO pathogenesis.

JQ5 but not JQ1 slows the progression of murine sclerodermatous cGVHD

To determine whether JQ5 or JQ1 could attenuate skin fibrosis in a murine sclerodermatous cGVHD model, B10.D2 BM and T cells were transplanted into minor histocompatibility antigen-disparate irradiated BALB/c recipients and monitored twice weekly for clinical and skin scores. Treatment was initiated once the average clinical scores were greater than 1 (day 20) and continued throughout study duration. Clinical scores were significantly lower within 20 days and skin scores within 10 days of JQ5 treatment versus vehicle controls (Figure 5A) without survival or weight improvement. In contrast, JQ1 did not reduce cutaneous disease severity and proved toxic to transplanted mice, with accelerated weight loss and mortality within

two weeks of initiating JQ1 treatment (Figure 5B). Day 45 images of JQ5 treated mice showed fewer and less severe skin lesions with JQ5 whereas day 28 images of JQ1 treated mice did not ameliorate sclerodermatous cGVHD. (Figure 5C).

Previously we reported that sclerodermatous cGVHD is Stat3-dependent and splenic T cells isolated from mice expressed the IFNγ and the Stat3-dependent cytokine IL17.[35] Inflammatory cytokine production measured in lymph node-derived T cells at study termination revealed JQ5 treatment significantly ($p<0.05$) reduced IL17 and IFNγ producing CD4+ T cell frequency (Figure 5D). Skin cryosections showed significantly diminished collagen deposition in the skin of JQ5 vs vehicle treated mice (Figures 5E and 5F). Together, these findings suggest that JQ5 has treatment potential for multiple cGVHD manifestations, whereas JQ1's potential appears limited to management of cGVHD/BO and not scleroderma.

JQ5 and JQ1 induce distinct transcriptional signatures in GCBs

JQ1 and JQ5 each were effective in cGVHD/BO, whereas only JQ5 was effective in sclerodermatous cGVHD. To investigate the mechanistic targets of each drug we sequenced the RNA of GCBs isolated from the spleens of cGVHD/BO mice 49 days post-transplant. After alignment and quantification, principal component analysis (PCA) was used to cluster samples. By limiting variance to the top 500 genes, PCA clustering cleanly segregated the different treatment conditions while explaining nearly half of the total variance in the dataset. Interestingly neither JQ1 nor JQ5 co-clustered with BM-Only samples while JQ1 clustered close to cGVHD (Figure 6A) suggesting that neither drug restored cGVHD GCBs to the state of BM-Only transplanted mice. This is further evident in differential gene expression (DGE) analysis. Each agent induced differentially significant (adjusted p-value <0.05, Log2 fold change >0.15)

changes in a relatively small number of genes ((JQ1 (40) and JQ5 (27)) (Figures 6B and 6C), the vast majority of which did not overlap with other treatment conditions (Figure 6D). While neither drug reverted the GCB transcriptome to a healthy BM-Only like state each drug imposed different changes in GCBs in cGVHD.

To determine how genetic processes involved in cGVHD/BO were impacted, we performed gene set enrichment analysis (GSEA) using the molecular signatures database (MsigDB) hallmark gene collections.[52] The resulting network map of enriched gene sets in the BM-Only vs cGVHD comparison demonstrated that multiple inflammatory signaling cascades (IFNγ inflammatory response, TNFα signaling) were enriched in cGVHD-derived GCBs. In contrast, pro-proliferative gene sets (mTORC1 signaling, Myc Targets) were enriched in GCBs of BM-Only transplanted mice (Figure 6E). These pro-proliferative pathways were similarly enriched in JQ5 treated samples. In contrast, these pathways were enriched in cGVHD compared to JQ1 treated samples, indicating JQ1 did not increase pro-proliferative pathway expression the way JQ5 did. (Figures 6F and 6H). With respect to the immune signaling pathways associated with cGVHD, both JQ5 and JQ1 reduced pathway enrichment (Figures 6G and 6H). Together these findings suggest that while neither drug restored GCBs to a BM-Only like transcriptome, immune signaling disruption in cGVHD GCBs provides a likely mechanism by which both drugs contribute to GC response impairment in cGVHD/BO mice, whereas JQ5 but not JQ1 restores pro-proliferative pathways closer to that observed in BM-Only GCBs.

Discussion

Here we demonstrated that small molecule inhibitors of epigenetic modifiers can disrupt the GC response and ameliorate cGVHD/BO. Within these findings we have expanded on the

promise of JQ1 demonstrating that while it may not be effective in all models, JQ1 treatment can ablate pulmonary dysfunction in cGVHD/BO. More critically we present the first *in vivo* therapeutic studies of the novel EZH2 inhibitor JQ5 which was able to reduce cGVHD incidence in both a BO and sclerodermatous murine model. While previous studies have investigated both EZH2 inhibition and BET bromodomain inhibition in aGVHD, acute and chronic GVHD have independent and significantly different underlying mechanisms and pathophysiology.[53] Research into the roles of these inhibitors as treatments for aGVHD has limited bearing on their impact in cGVHD. Furthermore, in aGVHD the mechanistic data on these types of inhibitors largely focused on their impacts to T cell apoptosis and how that can affect disease.[32,54] By contrast our studies focus on the role of EZH2 and BET inhibitors on the germinal center reaction. These key differences speak to the novelty of these findings, and their potential impact.

Chromatin modifying protein inhibitors have gained traction in the field of cancer treatment research where they are used to target the aberrant epigenetic landscape unique to cancer cells.[55] Our findings expand the scope of these drugs by demonstrating their potential impact in transplant biology,[29] and the proposition that mis-regulated biological processes in which their target enzymes are involved can be disrupted.[56–60]. Previous work on epigenetic targeting therapies in GVHD have shown that the DNA methyltransferase inhibitor Azacytidine (AzaC) was able to reduce GVHD in both murine and xenogeneic models.[61,62] Most notably the histone deacetylase inhibitor Vorinostat has shown success in a phase 2 clinical trial for aGVHD prevention.[63] Vorinostat and AzaC supported T regulatory cell expansion and Vorinostat additionally suppressed host antigen presenting cells and reduced Th1 and Th17 cells in aGVHD models.[62,64–66] In contrast to these earlier reports, we expand this strategy into cGVHD, looking

at both a separate mechanism, the germinal center, and two epigenetic modifications (H3K27Ac recognition, and H3K27me3 regulation) that have not been extensively studied in cGVHD.

Of the JQ5 inhibitors that we tested, only JQ5 was able to successfully treat murine cGVHD. In contrast, UNC1999 was highly toxic with 50% of treated mice dying within 2 days of initiating therapy, while DZNep had no observed impact on pulmonary function. These results are similar to what is observed in aGVHD models, where the EZH2 inhibitors GSK126 and EPZ6438, which specifically decrease H3K27me3 without affecting EZH2 protein, failed to prevent aGVHD, even though EZH2 genetic ablation in donor T cells reduced aGVHD severity.[67,68] This makes JQ5 uniquely able to recapitulate the improvements observed in EZH2 knockout models likely as a result of the compound specificity and mechanism. Unlike JQ5 which is highly specific to EZH2 and a direct competitive inhibitor for the binding of S-adenosyl-methionine (SAM)[69], DZNep impairs EZH2 indirectly by inhibiting AdoHcy cyclase to reduce the availability of SAM.[48,70] While UNC1999 is also an inhibitor of the binding of SAM it lacks the high specificity for EZH2 of JQ5.[71]

Both JQ1 and JQ5 successfully reduced the splenic frequency of GC cell populations, as well the GC frequency and size, correlating with a clear improvement in pulmonary function and adding to a growing body of evidence that the GC reaction plays a key role in the pathogenesis of cGVHD/BO generated under the conditions detailed here. By demonstrating that both drugs also reduced mature PC lung infiltration, a previously uninvestigated component of this mechanism, implicates PCs as potential contributors to cGVHD/BO pathogenesis. Other examples of successful pre-clinical drugs that treated murine cGVHD while impairing the GC response include pirfenidone (5-methyl-1-phenyl-2-[1H]-pyridone; SMAD2/3 inhibitor), ibrutinib (anti-BTK/ITK mAb), and Bcl-6 peptidomemitic inhibitor 79-6.[72–74]

In a high inflammatory sclerodermatous cGVHD model, JQ5 treatment reduced the formation of skin lesion in treated animals. Contrasting with its response in the cGVHD/BO model, JQ1 treatment proved toxic in this sclerodermatous model. We propose that JQ1 is not well tolerated under high inflammatory conditions as seen in the sclerodermatous model and in contrast to the low inflammatory conditions cGVHD/BO GVHD model. In support of that contention, we also tested the impact of JQ1 on an actual aGVHD model and observed accelerated lethality(data not shown).

Previous mechanistic insights from sequencing experiments on cGVHD are scarce. Although some single-cell capture and sequencing of samples from cGVHD patients has been performed, the emphasis has largely been on T cells and is limited to circulating cells.[75–77] Previous murine studies also focused primarily on the T cell population in cGVHD.[78,79] Herein we report the first detailed immune analyses coupled with transcriptomic in GCBs from cGVHD/BO mice. Interestingly, neither compound restored a BM Only (non-cGVHD control) transcriptomic state. Rather each compound induced a unique set of changes independently incompatible with GCBs function in cGVHD. Decreased pro-proliferative signaling expression in cGVHD relative to BM-Only GCBs is at first counterintuitive, as these pathways are essential for GC formation.[80] However, these findings may be a sign of active somatic hypermutation or class switch recombination in cGVHD GCBs, processes that can decrease proliferative signaling, consistent with elevated immune signaling observed in our analysis.[80,81] Both JQ5 and JQ1 lead to a reduction in the enrichment of several immune signaling pathways, especially IL2-STAT5 signaling and the inflammatory response, suggesting that these and not pro-proliferative pathways are critical for GC formation in cGVHD/BO mice. JQ1 did not impact genes

associated with proliferation such as mTORC1 signaling and cMyc targets, providing some mechanistic insight into the different impacts each drug has.

Taken together our results demonstrate the efficacy of targeted inhibition of epigenetic targets as a strategy for the treatment of cGVHD. Both the novel EZH2 inhibitor JQ5, and BET-bromodomain inhibitor JQ1 reduced the severity of pulmonary fibrosis from cGVHD/BO. Despite the distinct molecular mechanisms altered by JQ5 vs JQ1, each disrupted the GC reaction and reduced disease severity. As existing options for treatment of cGVHD remain limited, these studies provide a strong rational for future clinical investigation of bromodomain inhibitors and EZH2 inhibitors for treatment of cGVHD/BO (and of EZH2 inhibitors for the treatment of sclerodermatous cGVHD) as both types of compounds are either in clinical trial or approved by FDA.

Acknowledgments

This work was supported in part by National Institutes of Health National Cancer Institute (P01 CA142106), National Institute of Allergy and Infectious Disease grants (P01 AI56299; T32 AI007313, R01 CA222218), Leukemia Society of America Translational Research Grant 6458-15, and the Children's' Cancer Research Fund.

Authorship Contributions:

M.Z. designed experiments, performed experiments, and wrote the paper. R.F. Designed and performed experiments. K.P., S.R., S.J., F.M., S.A., and G.T., performed and assisted with experiments. P.M.P., M.L.H., P.T.S., L.S.K. assisted with bioinformatic analyses. J.Q., J.E.B., synthesized and provided reagents and discussed experiments. J.A.B. and M. DuPage provided

mice for experiments. A.H.S., C.S.C., J.K, J.H.A., R.J.S., J.R., L.L., I.M., G.R.H, K.P.M, D.H.M., J.S.S, W.J.M., Y.Z. discussed experiments, results, and conclusions. J.Q., B.R.B designed experiments, reviewed data, and assisted in manuscript preparation. All authors edited the manuscript.

Conflict of Interest Disclosures:

BRB receives remuneration as an advisor to Magenta Therapeutics and BlueRock Therapeutics; Research funding from BlueRock Therapeutics, Rheos Medicines, Equilibre biopharmaceuticals, Carisma Therapeutics, Inc., and is a co-founder of Tmunity Therapeutics. JQ is a scientific co-founder and consultant for Epiphanes; and consultant for Talus. GRH has consulted for Generon Corporation, NapaJen Pharma, iTeos Therapeutics, Neoleukin Therapeutics and has received research funding from Compass Therapeutics, Syndax Pharmaceuticals, Applied Molecular Transport, Serplus Technology, Heat Biologics, Laevoroc Oncology and iTeos Therapeutics.

References

1. Greinix HT. Chronic GVHD: Progress in salvage treatment? *Blood*. 2017;130(21):2237–2238.
2. Flowers MED, Parker PM, Johnston LJ, et al. Comparison of chronic graft-versus-host disease after transplantation of peripheral blood stem cells versus bone marrow in allogeneic recipients: Long-term follow-up of a randomized trial. *Blood*. 2002;100(2):415–419.
3. Lee SJ. Have we made progress in the management of chronic graft-vs-host disease? *Best Practice and Research: Clinical Haematology*. 2010;23(4):529–535.
4. Socié G, Stone JV, Wingard JR, et al. Long-Term Survival and Late Deaths after Allogeneic Bone Marrow Transplantation. *New England Journal of Medicine*. 1999;341(1):14–21.
5. Lee SJ, Klein JP, Barrett AJ, et al. Severity of chronic graft-versus-host disease: Association with treatment-related mortality and relapse. *Blood*. 2002;100(2):406–414.

6. Miklos D, Cutler CS, Arora M, et al. Ibrutinib for chronic graft-versus-host disease after failure of prior therapy. *Blood*. 2017;130(21):2243–2250.
7. Wolff D, Gerbitz A, Ayuk F, et al. Consensus conference on clinical practice in chronic graft-versus-host disease (GVHD): First-line and topical treatment of chronic GVHD. *Biology of Blood and Marrow Transplantation*. 2010;16(12):1611–1628.
8. Jagasia M, Lazaryan A, Bachier CR, et al. ROCK2 inhibition with belumosudil (KD025) for the treatment of chronic graft-versus-host disease. *Journal of Clinical Oncology*. 2021;39(17):1888–1898.
9. Zeiser R, Polverelli N, Ram R, et al. Ruxolitinib for Glucocorticoid-Refractory Chronic Graft-versus-Host Disease. *New England Journal of Medicine*. 2021;385(3):228–238.
10. Mawardi H, Hashmi SK, Elad S, Aljurf M, Treister N. Chronic graft-versus-host disease: Current management paradigm and future perspectives. *Oral Diseases*. 2018;25(June):1–18.
11. Hildebrandt GC, Fazekas T, Lawitschka A, et al. Diagnosis and treatment of pulmonary chronic GVHD: Report from the consensus conference on clinical practice in chronic GVHD. *Bone Marrow Transplantation*. 2011;46(10):1283–1295.
12. Flynn R, Paz K, Du J, et al. Targeted Rho-associated kinase 2 inhibition suppresses murine and human chronic GVHD through a Stat3-dependent mechanism. *Blood*. 2016;127(17):2144–2154.
13. Jagasia M, Salhotra A, Bachier CR, et al. KD025-208: A Phase 2a Study of KD025 for Patients with Chronic Graft Versus Host Disease (cGVHD) - Pharmacodynamics (PD) and Updated Results. *Biology of Blood and Marrow Transplantation*. 2019;25(3):S28–S29.
14. Panoskaltsis-Mortari A, Tram K V., Price AP, Wendt CH, Blazar BR. A new murine model for bronchiolitis obliterans post-bone marrow transplant. *American Journal of Respiratory and Critical Care Medicine*. 2007;176(7):713–723.
15. Srinivasan M, Flynn R, Price A, et al. Donor B-cell alloantibody deposition and germinal center formation are required for the development of murine chronic GVHD and bronchiolitis obliterans. *Blood*. 2012;119(6):1570–1580.
16. Flynn R, Du J, Veenstra RG, et al. Increased T follicular helper cells and germinal center B cells are required for cGVHD and bronchiolitis obliterans. *Blood*. 2014;123(25):3988–3998.
17. Béguelin W, Popovic R, Teater M, et al. EZH2 Is Required for Germinal Center Formation and Somatic EZH2 Mutations Promote Lymphoid Transformation. *Cancer Cell*. 2013;23(5):677–692.
18. Velichutina I, Shaknovich R, Geng H, et al. EZH2-mediated epigenetic silencing in germinal center B cells contributes to proliferation and lymphomagenesis. *Blood*. 2010;116(24):5247–5255.
19. Czermin B, Melfi R, McCabe D, et al. Drosophila enhancer of Zeste/ESC complexes have a histone H3 methyltransferase activity that marks chromosomal Polycomb sites. *Cell*. 2002;111(2):185–196.
20. Cao R, Wang L, Wang H, et al. Role of histone H3 lysine 27 methylation in polycomb-group silencing. *Science*. 2002;298(5595):1039–1043.
21. Boyer LA, Plath K, Zeitlinger J, et al. Polycomb complexes repress developmental regulators in murine embryonic stem cells. *Nature*. 2006;441(7091):349–353.

22. Lee TI, Jenner RG, Boyer LA, et al. Control of Developmental Regulators by Polycomb in Human Embryonic Stem Cells. *Cell*. 2006;125(2):301–313.
23. Bernstein BE, Mikkelsen TS, Xie X, et al. A Bivalent Chromatin Structure Marks Key Developmental Genes in Embryonic Stem Cells. *Cell*. 2006;125(2):315–326.
24. Shin DM, Liu R, Wu W, et al. Global gene expression analysis of very small embryonic-like stem cells reveals that the Ezh2-dependent bivalent domain mechanism contributes to their pluripotent state. *Stem Cells and Development*. 2012;21(10):1639–1652.
25. Li B, Chng WJ. EZH2 abnormalities in lymphoid malignancies: Underlying mechanisms and therapeutic implications. *Journal of Hematology and Oncology*. 2019;12(1):1–13.
26. Teresa Villanueva M. Anticancer drugs: All roads lead to EZH2 inhibition. *Nature Reviews Drug Discovery*. 2017;16(4):239.
27. Tan JZ, Yan Y, Wang XX, Jiang Y, Xu HE. EZH2: Biology, disease, and structure-based drug discovery. *Acta Pharmacologica Sinica*. 2014;35(2):161–174.
28. Filippakopoulos P, Qi J, Picaud S, et al. Selective inhibition of BET bromodomains. *Nature*. 2010;468(7327):1067–1073.
29. Alqahtani A, Choucair K, Ashraf M, et al. Bromodomain and extra-terminal motif inhibitors: A review of preclinical and clinical advances in cancer therapy. *Future Science OA*. 2019;5(3):.
30. Mele DA, Salmeron A, Ghosh S, et al. BET bromodomain inhibition suppresses TH17-mediated pathology. *Journal of Experimental Medicine*. 2013;210(11):2181–2190.
31. Gao F, Yang Y, Wang Z, Gao X, Zheng B. BRAD4 plays a critical role in germinal center response by regulating Bcl-6 and NF-κB activation. *Cellular Immunology*. 2015;294(1):1–8.
32. Y. S, Y. W, T. T, et al. BET bromodomain inhibition suppresses graft-versus-host disease after allogeneic bone marrow transplantation in Mice. *Blood*. 2015;125(17):2724–2728.
33. Wang D, Quiros J, Mahuron K, et al. Targeting EZH2 Reprograms Intratumoral Regulatory T Cells to Enhance Cancer Immunity. *Cell Reports*. 2018;23(11):3262–3274.
34. DuPage M, Chopra G, Quiros J, et al. The chromatin-modifying enzyme Ezh2 is critical for the maintenance of regulatory T cell identity after activation. *Immunity*. 2015;42(2):227–238.
35. Radojcic V, Pletneva MA, Yen H-R, et al. STAT3 Signaling in CD4 + T Cells Is Critical for the Pathogenesis of Chronic Sclerodermatous Graft-Versus-Host Disease in a Murine Model . *The Journal of Immunology*. 2010;184(2):764–774.
36. Anderson BE, McNiff J, Yan J, et al. Memory CD4+ T cells do not induce graft-versus-host disease. *Journal of Clinical Investigation*. 2003;112(1):101–108.
37. Zhang H, Qi J, Reyes JM, et al. Oncogenic deregulation of EZH2 as an opportunity for targeted therapy in lung cancer. *Cancer Discovery*. 2016;6(9):1007–1021.
38. Pau G, Fuchs F, Sklyar O, Boutros M, Huber W. EBImage-an R package for image processing with applications to cellular phenotypes. *Bioinformatics*. 2010;26(7):979–981.
39. Blazar BR, Taylor PA, McElmurry R, et al. Engraftment of Severe Combined Immune Deficient Mice Receiving Allogeneic Bone Marrow Via In Utero or Postnatal Transfer. *Blood*. 1998;92(10):3949–3959.
40. Baller J, Kono T, Herman A, Zhang Y. ChURP: A lightweight CLI framework to enable novice users to analyze sequencing datasets in parallel. *ACM International Conference Proceeding Series*. 2019;

41. Anders S. Babraham Bioinformatics - FastQC A Quality Control tool for High Throughput Sequence Data. *Soil*. 2010;5(1):.
42. Bolger AM, Lohse M, Usadel B. Trimmomatic: A flexible trimmer for Illumina sequence data. *Bioinformatics*. 2014;30(15):2114–2120.
43. Kim D, Paggi JM, Park C, Bennett C, Salzberg SL. Graph-based genome alignment and genotyping with HISAT2 and HISAT-genotype. *Nature Biotechnology 2019 37:8*. 2019;37(8):907–915.
44. Danecek P, Bonfield JK, Liddle J, et al. Twelve years of SAMtools and BCFtools. *GigaScience*. 2021;10(2):.
45. Liao Y, Smyth GK, Shi W. FeatureCounts: An efficient general purpose program for assigning sequence reads to genomic features. *Bioinformatics*. 2014;30(7):923–930.
46. Love MI, Huber W, Anders S. Moderated estimation of fold change and dispersion for RNA-seq data with DESeq2. *Genome Biology*. 2014;15(12):1–21.
47. Konze KD, Ma A, Li F, et al. An orally bioavailable chemical probe of the lysine methyltransferases EZH2 and EZH1. *ACS Chemical Biology*. 2013;8(6):1324–1334.
48. Miranda TB, Cortez CC, Yoo CB, et al. DZNep is a global histone methylation inhibitor that reactivates developmental genes not silenced by DNA methylation. *Molecular Cancer Therapeutics*. 2009;8(6):1579–1588.
49. Sinha RK, Flynn R, Zaiken M, et al. Activated protein C ameliorates chronic graft-versus-host disease by PAR1-dependent biased cell signaling on T cells. *Blood*. 2019;134(9):776–781.
50. Reynaud-Gaubert M, Thomas P, Badier M, et al. Early Detection of Airway Involvement in Obliterative Bronchiolitis after Lung Transplantation. *https://doi.org/10.1164/ajrccm.161.6.9905060*. 2012;161(6):1924–1929.
51. Sarantopoulos S, Blazar BR, Cutler C, Ritz J. B Cells in Chronic Graft-versus-Host Disease. *Biology of Blood and Marrow Transplantation*. 2015;21(1):16–23.
52. Liberzon A, Birger C, Thorvaldsdóttir H, et al. The Molecular Signatures Database Hallmark Gene Set Collection. *Cell Systems*. 2015;1(6):417–425.
53. Blazar BR, Murphy WJ, Abedi M. Advances in graft-versus-host disease biology and therapy. *Nature Reviews Immunology*. 2012;12(6):443–458.
54. Kamijo H, Sugaya M, Takahashi N, et al. BET bromodomain inhibitor JQ1 decreases CD30 and CCR4 expression and proliferation of cutaneous T-cell lymphoma cell lines. *Archives of dermatological research*. 2017;309(6):491–497.
55. Berdasco M, Esteller M. Aberrant Epigenetic Landscape in Cancer: How Cellular Identity Goes Awry. *Developmental Cell*. 2010;19(5):698–711.
56. Chen H, Liu H, Qing G. Targeting oncogenic Myc as a strategy for cancer treatment. *Signal Transduction and Targeted Therapy*. 2018;3(1):.
57. Mertz JA, Conery AR, Bryant BM, et al. Targeting MYC dependence in cancer by inhibiting BET bromodomains. *Proceedings of the National Academy of Sciences of the United States of America*. 2011;108(40):16669–16674.
58. Zuber J, Shi J, Wang E, et al. RNAi screen identifies Brd4 as a therapeutic target in acute myeloid leukaemia. *Nature*. 2011;478(7370):524–528.
59. Stewart HJS, Horne GA, Bastow S, Chevassut TJT. BRD4 associates with p53 in DNMT3A-mutated leukemia cells and is implicated in apoptosis by the bromodomain inhibitor JQ1. *Cancer Medicine*. 2013;2(6):826–835.

60. Dawson MA, Prinjha RK, Dittmann A, et al. Inhibition of BET recruitment to chromatin as an effective treatment for MLL-fusion leukaemia. *Nature*. 2011;478(7370):529–533.
61. Ehx G, Fransolet G, de Leval L, et al. Azacytidine prevents experimental xenogeneic graft-versus-host disease without abrogating graft-versus-leukemia effects. *OncoImmunology*. 2017;6(5):1–14.
62. Cooper ML, Choi J, Karpova D, et al. Azacitidine Mitigates Graft-versus-Host Disease via Differential Effects on the Proliferation of T Effectors and Natural Regulatory T Cells In Vivo. *The Journal of Immunology*. 2017;198(9):3746–3754.
63. Choi SW, Braun T, Henig I, et al. Vorinostat plus tacrolimus/methotrexate to prevent GVHD after myeloablative conditioning, unrelated donor HCT. *Blood*. 2017;130(15):1760–1767.
64. Holtan SG, Weisdorf DJ. Vorinostat is victorious in GVHD prevention. *Blood*. 2017;130(15):1690–1691.
65. Cho S, Reddy P. HDAC inhibition and graft versus host disease. *Molecular Medicine*. 2011;17(5–6):404–416.
66. Reddy P, Maeda Y, Hotary K, et al. Histone deacetylase inhibitor suberoylanilide hydroxamic acid reduces acute graft-versus-host disease and preserves graft-versus-leukemia effect. *Proceedings of the National Academy of Sciences of the United States of America*. 2004;101(11):3921–3926.
67. Huang Q, He S, Tian Y, et al. Hsp90 inhibition destabilizes Ezh2 protein in alloreactive T cells and reduces graft-versus-host disease in mice. *Blood*. 2017;129(20):2737–2748.
68. Alahmari B, Cooper M, Ziga E, et al. Selective targeting of histone modification fails to prevent graft versus host disease after hematopoietic cell transplantation. *PloS one*. 2018;13(11):e0207609.
69. Souroullas GP, Jeck WR, Parker JS, et al. An oncogenic Ezh2 mutation induces tumors through global redistribution of histone 3 lysine 27 trimethylation. *Nature Medicine*. 2016;22(6):632–640.
70. Tan J, Yang X, Zhuang L, et al. Pharmacologic disruption of polycomb-repressive complex 2-mediated gene repression selectively induces apoptosis in cancer cells. *Genes and Development*. 2007;21(9):1050–1063.
71. Konze KD, Ma A, Li F, et al. An orally bioavailable chemical probe of the lysine methyltransferases EZH2 and EZH1. *ACS Chemical Biology*. 2013;8(6):1324–1334.
72. Du J, Paz K, Flynn R, et al. Pirfenidone ameliorates murine chronic GVHD through inhibition of macrophage infiltration and TGF-β production. *Blood*. 2017;129(18):2570–2580.
73. Paz K, Flynn R, Du J, et al. Small-molecule BCL6 inhibitor effectively treats mice with nonsclerodermatous chronic graft-versus-host disease. *Blood*. 2019;133(1):94–99.
74. Dubovsky JA, Flynn R, Du J, et al. Ibrutinib treatment ameliorates murine chronic graft-versus-host disease. *Journal of Clinical Investigation*. 2014;124(11):4867–4876.
75. Balakrishnan A, Gloude N, Sasik R, Ball ED, Morris GP. Proinflammatory Dual Receptor T Cells in Chronic Graft-versus-Host Disease. *Biology of Blood and Marrow Transplantation*. 2017;23(11):1852–1860.
76. Santos E Sousa P, Ciré S, Conlan T, et al. Peripheral tissues reprogram CD8+ T cells for pathogenicity during graft-versus-host disease. *JCI insight*. 2018;3(5):.

77. Poe JC, Zhang D, Xie J, et al. Single-Cell RNA-Seq Identifies Potentially Pathogenic B Cell Populations That Uniquely Circulate in Patients with Chronic Gvhd. *Blood*. 2019;134(Supplement_1):874–874.
78. Zhong H, Liu Y, Xu Z, et al. TGF-β-induced CD8+CD103+ regulatory T cells show potent therapeutic effect on chronic graft-versus-host disease lupus by suppressing B cells. *Frontiers in Immunology*. 2018;9(JAN):35.
79. Deng R, Hurtz C, Song Q, et al. Extrafollicular CD4+ T-B interactions are sufficient for inducing autoimmune-like chronic graft-versus-host disease. *Nature Communications*. 2017;8(1):1–17.
80. Calado DP, Sasaki Y, Godinho SA, et al. The cell-cycle regulator c-Myc is essential for the formation and maintenance of germinal centers. *Nature Immunology*. 2012;13(11):1092–1100.
81. Klein U, Dalla-Favera R. Germinal centres: Role in B-cell physiology and malignancy. Nat Rev Immunol; 2008.

Figure Legends

Figure 1: JQ5 and JQ1 treat murine cGVHD/BO. Results are from BO cGVHD transplants. B10.BR mice were conditioned 120mg/kg Cytoxan (days -3,-2) and 7.6 Gy total body irradiation (TBI) (day -1). On day 0 recipients received $10x10^6$ purified BM cells ± $73.5x10^3$ B6 purified T cells from C57BL/6. Groups included a BM Only negative control, a WT BM and T Cell positive control, and mice that were given each treatment either JQ5 (75mg/kg 3x/week) or JQ1 (50mg/kg 3x/week) from day 28 to day 49 post-transplant. Results shown are pooled from three transplant replicates. (A-B) Results of pulmonary function tests taken on day 49 post-transplant include measures of resistance, elastance, and compliance. Significant improvement in pulmonary function across multiple parameters was observed with both JQ5 ((n = 22/BM Only, n=17/cGVHD, n = 15/JQ5) (A) and JQ1 (n=18/BM Only, n=20/cGVHD, n=18/JQ1) (B) treatment. (C-F) Representative images of cryopreserved lung sections from mice 49 days post-transplant. (C-D) Sections were stained with Masson's Trichrome and analyzed for collagen deposition. Quantification of the trichrome positive area is in the right most panel. This deposition is significantly reduced in both the JQ5 treated mice (n=8/BM Only, n=11/cGVHD,

n=8/JQ5) (C) and the JQ1 treated mice (n=7/BM Only, n= 8/cGVHD, n=8/JQ1) (D). (E-F) Sections were stained with anti IgG FITC and DAPI and show a reduction of IgG+ tissue in both JQ5 treated mice (n=5/BM Only, n=5/cGVHD, n=4/JQ5) (E) and the JQ1 treated mice (n=5/BM Only, n=5/cGVHD, n=4/JQ1) (F). Quantification of FITC+ area is shown in right most panels. All images are at 200x magnification. Statistics shown are results of unpaired t-test with Bonferroni corrected p-values when appropriate. *<0.05, **<0.01, ***<0.001, ****<0.0001.

Figure 2: JQ1 and JQ5 impair the GC reaction in murine cGVHD/BO mice. (A-I) Transplants were performed as in Figure 1; groups are as defined in Figure 1. Results shown are pooled from three transplant replicates (A-C) Flow cytometry analysis of mouse splenocytes taken 49 days post-transplant. TFH frequency is defined as % CXCR5+, PD1+ of FoxP3-, CD4+ live splenocytes. TFRs are the CXCR5+, PD1+ percentage of FoxP3+, CD4+ live splenocytes. The TFR/TFH ratio is shown. GCBs are GL7+, FAS^{hi} percentage of the CD19+ live splenocytes. (A) JQ5 treatment resulted in a significant decrease in TFH and GCB frequencies and increase in TFR frequency and the TFR/TFH ratio (n= 23/BM Only, n= 18/cGVHD, n=15/JQ5). (B) Similar results are shown for each population with JQ1 treatment, consistent with reduced GC reaction (n=14/BM Only, n=11/cGVHD, n=7/JQ1). (C) Representative gating for TFH and TFR cells (Left) and GCB cells (Right). BM Only contours are in blue, cGVHD contours are in red. (D) Representative images of cryopreserved spleen sections stained to show GCs from mice 49 days post-transplant. Sections are stained with DAPI (blue), PNA rhodamine (red), and CD4 FITC (green). Images are at 200x magnification. (E-F) Left panel shows the number of GCs observed in each spleen section normalized for the area of spleen in each section. A GC was counted if it was a roughly circular region of PNA+ cells near a region of CD4+ cells. Right panel is a

quantification of the average size of GCs observed in each section. The GC size was determined as the area of the PNA+ region. For both JQ5 (n=8/BM Only, n=6/cGVHD, n=5/JQ5) (E) and JQ1 (n=5/group) (F) there was a significant reduction in both GC count and average size. (G) Flow cytometric analysis of single cell lung suspensions taken from transplanted mice treated with each drug (n=5/group). Total plasma cells (Left) are CD138+ lymphocytes, immature plasma cells (Middle) are B220+, CD19+ plasma cells, and mature plasma cells (Right) are B220-, CD19- plasma cells. Results show that both drugs significantly reduced the proportion of mature plasma cells in subject lungs. (H) Mean fluorescence intensity (MFI) quantification of flow cytometry analysis of H3K27me3 content of GC cell populations gated as in C (n per group as in panel A). (I) Representative histograms of GCB cells H3K27me3 content for BM Only, cGVHD, and JQ5 treated mouse derived cells. For all panels, statistics shown are results of unpaired t-test with Bonferroni corrected p-values, where appropriate. *<0.05, **<0.01, ***<0.001, ****<0.0001.

Figure 3: EZH2 expression in both donor T cells and B cells is necessary for cGVHD/BO (A-D) Mice were transplanted as in Figure 1. Groups shown are defined by the contents of the graft given on day 0. BM (EZH2 KO) refers to T cell depleted BM from B6 EZH2 fl/fl CD19-Cre mice. T (EZH2 KO) refers to purified T cells from B6 EZH2 fl/fl CD4 Cre mice. Results shown are pooled from two transplant replicates. (A-B) Results of pulmonary function tests on mice 49 days post-transplant, show significant improvement in pulmonary function if BM (A) or T cells (B) are obtained from EZH2 KO donors (n=7/BM Only, n=9/cGVHD, n=7/BM(EZH2 KO) Only, n=9/ BM(EZH2 KO) + T(WT), n=6/BM(WT) + T(EZH2 KO)). (C/E) Representative images of cryopreserved lung sections from mice 49 days post-transplant (n=4/BM Only,

n=6/cGVHD, n=4/BM(EZH2 KO) Only, n=8/BM(EZH2 KO) + T(WT), n=5/BM(WT) + T(EZH2 KO)). Sections were stained with Masson's Trichrome and analyzed for collagen deposition which is significantly reduced in recipients of T cells or BM from EZH2 KO donors. (D/F). Representative images of cryopreserved lung sections from mice 49 days post-transplant (n=5/BM Only, n=8/cGVHD, n=4/BM(EZH2 KO) Only, n=6/BM(EZH2 KO) + T(WT), n= BM(WT) + T(EZH2 KO)). Sections were stained with anti IgG FITC and DAPI and show reduction of IgG+ tissue in both the EZH2 KO T cell and EZH2 KO BM transplanted samples. Quantification of FITC+ area is shown in C. All images are at 200x magnification. Quantification of trichrome+ area is shown in the left panel of D. Statistics shown are results of unpaired t-test with Bonferroni corrected p-values when appropriate. *<0.05, **<0.01, ***<0.001, ****<0.0001.

Figure 4: In BO cGVHD EZH2 is necessary for the GC reaction. (A-D) Transplants were performed as in Figure 1; groups are as defined in Figure 3. (A-B) Flow cytometry analysis of mouse splenocytes taken 49 days post-transplant. Cell populations for flow cytometry analysis are as defined in Figure 2. Results show that when EZH2 is knocked out in both the BM compartment (A) (n=4/group) and T cell compartment (B) (n=14/BM Only, n=13/cGVHD, n=10/BM(WT) + T(EZH2 KO)) of the graft there is a significant reduction in the TFH and GCB frequencies, and a significant increase in the TFR/TFH ratio. (C) Representative images of cryopreserved spleen sections stained to show GCs from mice 49 days post-transplant. . Sections are stained with DAPI (blue), PNA rhodamine (red), and CD4 FITC (green). Images are at 200x magnification. . (D) Left panel shows the number of GCs observed in each spleen section normalized for the area of spleen in each section. Right panel is a quantification of the average

size of GCs observed in each section. GCs were identified and quantified as in Figure 2. Quantification shows when EZH2 is knocked out in either the BM and T cell compartments there is a comparable reduction in both the GC count and average size. N=8/BM Only, n=6/cGVHD, n=5/BM(EZH2 KO) Only, n=4/BM(EZH2 KO) + T(WT), n=4/BM(WT) + T(EZH2 KO). For all panels, statistics shown are results of unpaired t-test with Bonferroni corrected p-values, where appropriate. *<0.05, **<0.01, ***<0.001, ****<0.0001.

Figure 5: Treatment with JQ5, but not JQ1, can treat sclerodermatous cGVHD. (A-C) BALB/c mice were given TBI (700 cGy on day -1) followed by infusion of 10^7 B10.D2 BM plus or minus 1.8×10^6 CD4 and 0.9×10^6 CD8 T cells (day 0). JQ5 and JQ1 treated mice received treatment as in Figure 1 from days 20-45 post-transplant, n=25/group. (A-B) From left to right graphs show impact of JQ5 treatment on recipient survival, mean weights, clinical scores, and skin scores. Arrows on clinical and skin score plots indicate time of treatment initiation. (A) While JQ5 did not significantly improve either weights or survival proportion, treated mice showed significantly reduced clinical scores, and skin scores as early as 10 days after initial treatment. (B) JQ1 treatment shows evidence of toxicity within 7 days of beginning therapy with no mice surviving beyond two weeks after treatment initiation. (C) Representative images of sclerodermatous mice with or without treatment with each drug. Images taken 45 days post-transplant, except for JQ1 treated mouse where image was taken 34 days post-transplant. (D) Flow cytometry analysis of cytokine production from transplanted mouse lymph nodes, shows a significant reduction in inflammatory cytokine production with JQ5 treatment, indicative of reduced disease, n=5/group. (E) Representative images of cryopreserved skin cross sections from mice 45 days post-transplant. Sections were stained with Masson's Trichrome. Images are at

200x magnification. (F) Quantification of Trichrome+ area of skin cross sections in C, shows a significant reduction in trichrome positive area with JQ5 treatment, n=4/group. This correlates to a reduction in skin collagen deposition with treatment. *<0.05, **<0.01, ***<0.001, ****<0.0001.

Figure 6: JQ5 and JQ1 impair GCB cells through distinct transcriptomic signatures. All results from analysis of sorted GCBs collected ~49 days post-transplant in cGVHD/BO B6→B10.BR model. 4 samples in each group are used for analysis, samples were chosen to be most representative of each treatment condition by pulmonary function test results. (A) Principal component analysis (PCA) of top 4 samples in each treatment condition, calculated with top 500 most variable genes. Treatment condition variation along the top two principal components explains ~48% of variance within the dataset. All groups cluster independently. (B-C) Volcano plot of differentially expressed genes in either (A) JQ1 or (B) JQ5 treated samples against vehicle treated (cGVHD) samples. Differentially expressed genes called as having an adjusted p value less than 0.05, and a log2 fold change greater than 0.15. Twenty-four genes were differentially increased and sixteen were reduced with JQ1, and eight genes were differentially increased and nineteen were reduced with JQ5. (D) Euler plots of overlapping differentially expressed genes in each of the four treatment conditions. Left plot is upregulated genes, while right is downregulated genes. (E) GSEA network mapping of MsigDB hallmark gene sets in BM Only vs cGVHD comparison. Red nodes were increased with cGVHD vs BM Only samples, blue nodes were decreased. (F-G) Individual enrichment barcode plots for (F left to right) MTORC1 signaling, Myc targets V1, oxidative phosphorylation, (G left to right) allograft rejection, IL2-STAT5 signaling, and inflammatory response hallmark gene sets. On all plot's

genes enriched in the treatment condition are on the left while genes enriched in cGVHD are on the right. Gene sets in E JQ5 and JQ1 impacted enrichment differently, gene sets in F sets were enriched comparably. (H) Heatmap of high variance genes in major GSEA nodes described in D. In A,C,F, and G colors defined as blue for BM Only, red for cGVHD, black for JQ5 treated, and green for JQ1 treated.

Figure 1:

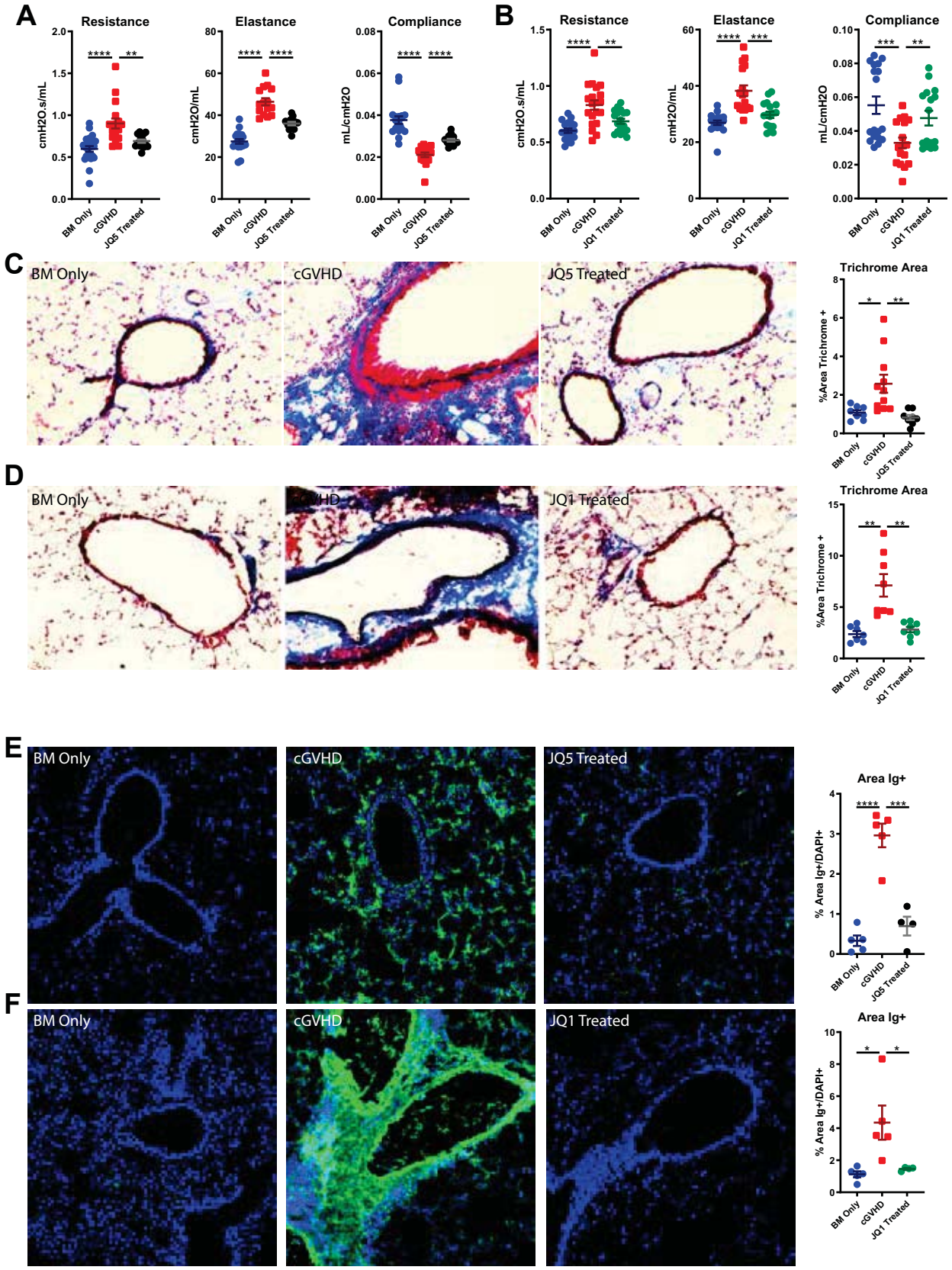
A
Resistance
Elastance
Compliance
cmH2O.s/mL
cmH2O/mL
mL/cmH2O
BM Only
cGVHD
JQ5 Treated
B
Resistance
Elastance
Compliance
cmH2O.s/mL
cmH2O/mL
mL/cmH2O
BM Only
cGVHD
JQ1 Treated
C
BM Only
cGVHD
JQ5 Treated
Trichrome Area
%Area Trichrome +
D
BM Only
cGVHD
JQ1 Treated
Trichrome Area
%Area Trichrome +
E
BM Only
cGVHD
JQ5 Treated
Area Ig+
% Area Ig+/DAPI+
F
BM Only
cGVHD
JQ1 Treated
Area Ig+
% Area Ig+/DAPI+

Figure 2:

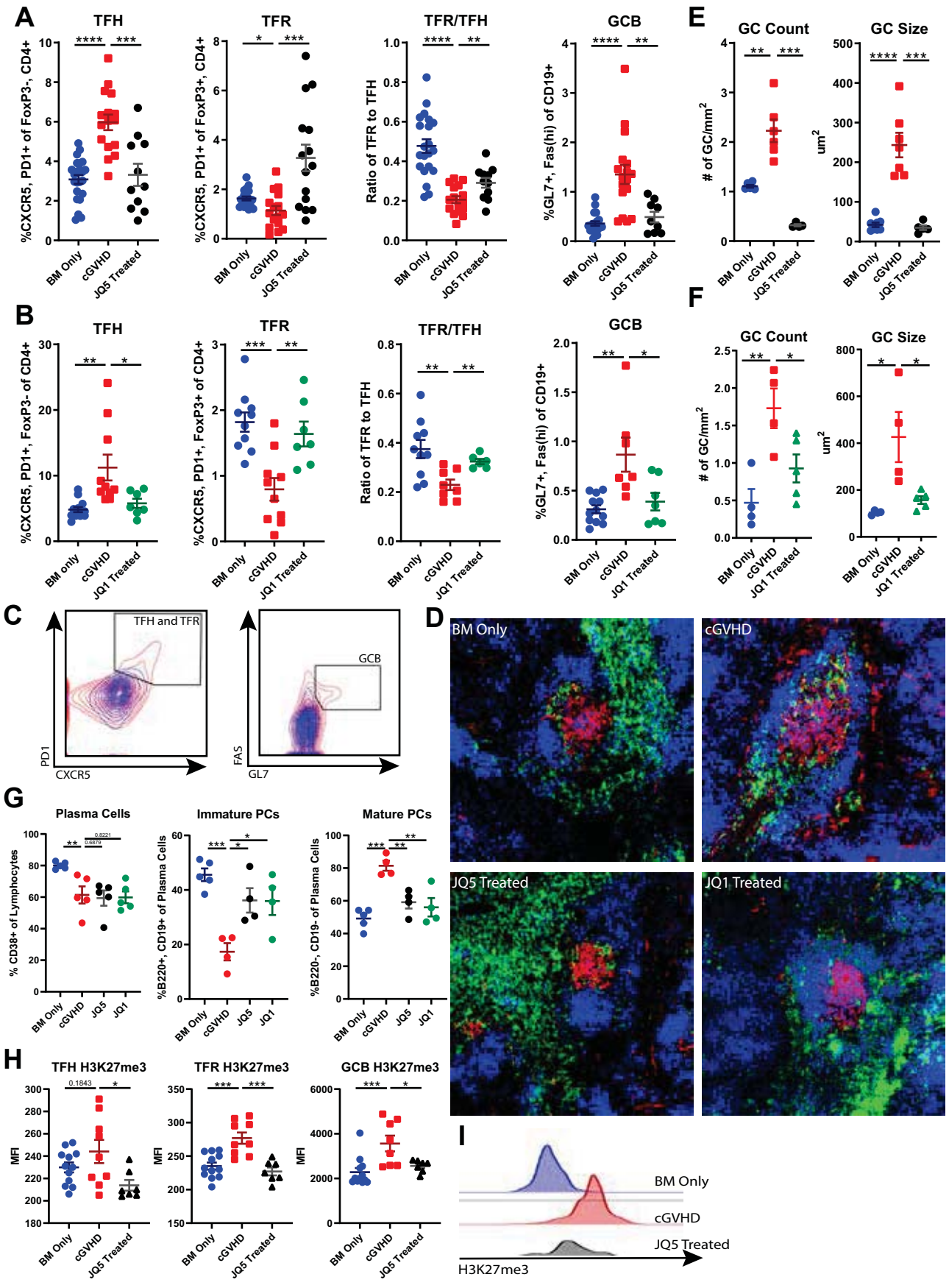
A
TFH
%CXCR5, PD1+ of FoxP3-, CD4+
TFR
%CXCR5, PD1+ of FoxP3+, CD4+
TFR/TFH
Ratio of TFR to TFH
GCB
%GL7+, Fas(hi) of CD19+
BM Only
cGVHD
JQ5 Treated
E
GC Count
# of GC/mm2
GC Size
um2
B
TFH
%CXCR5, PD1+, FoxP3- of CD4+
TFR
%CXCR5, PD1+, FoxP3+ of CD4+
TFR/TFH
Ratio of TFR to TFH
GCB
%GL7+, Fas(hi) of CD19+
BM only
cGVHD
JQ1 Treated
F
GC Count
# of GC/mm2
GC Size
um2
C
TFH and TFR
PD1
CXCR5
GCB
FAS
GL7
D
BM Only
cGVHD
JQ5 Treated
JQ1 Treated
G
Plasma Cells
% CD38+ of Lymphocytes
Immature PCs
%B220+, CD19+ of Plasma Cells
Mature PCs
%B220-, CD19- of Plasma Cells
BM Only
cGVHD
JQ5
JQ1
H
TFH H3K27me3
TFR H3K27me3
GCB H3K27me3
MFI
BM Only
cGVHD
JQ5 Treated
I
BM Only
cGVHD
JQ5 Treated
H3K27me3

Figure 3:

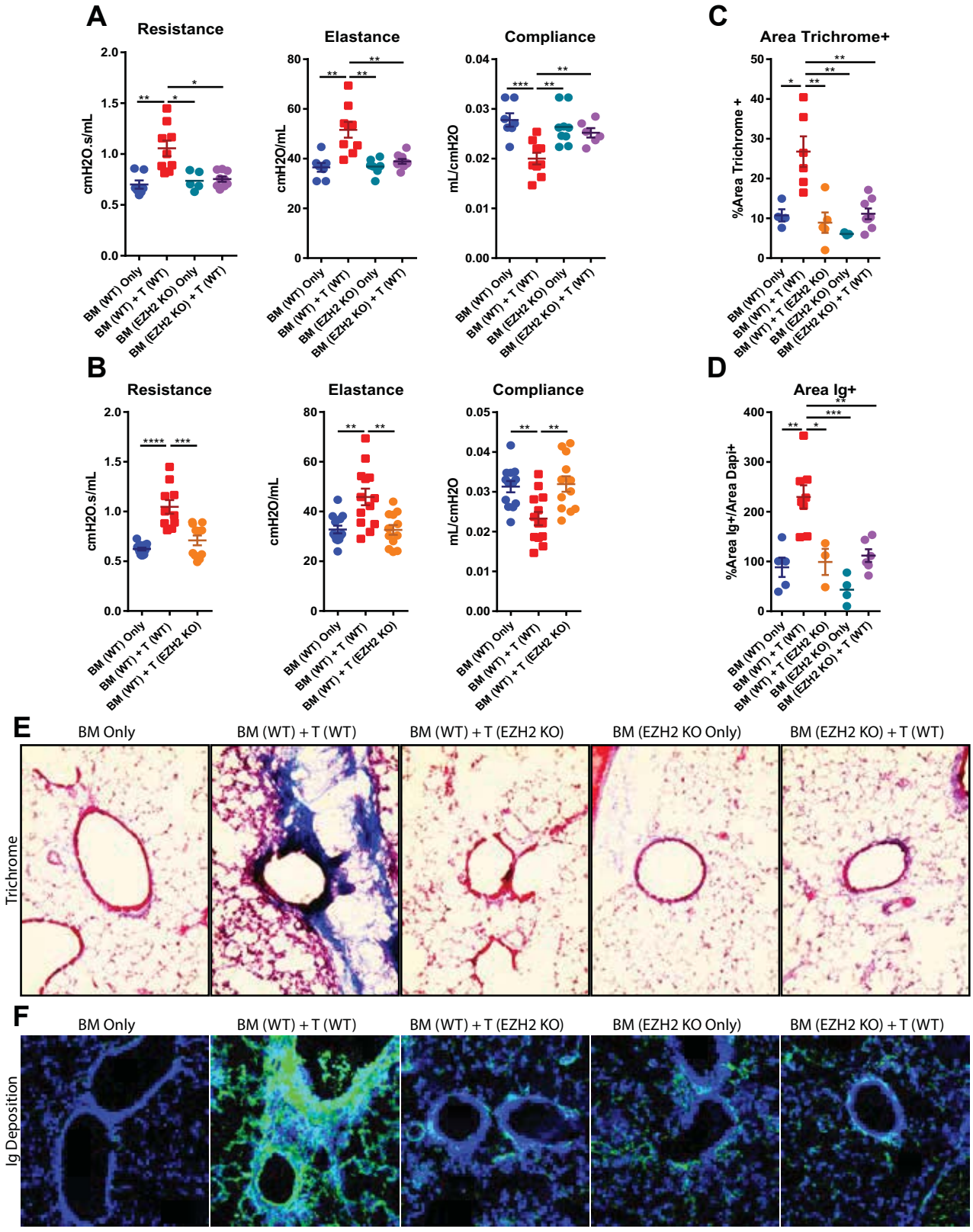
A
Resistance
cmH2O.s/mL
Elastance
cmH2O/mL
Compliance
mL/cmH2O
C
Area Trichrome+
%Area Trichrome +
BM (WT) Only
BM (WT) + T (WT)
BM (EZH2 KO) Only
BM (EZH2 KO) + T (WT)
B
Resistance
Elastance
Compliance
BM (WT) Only
BM (WT) + T (WT)
BM (WT) + T (EZH2 KO)
D
Area Ig+
%Area Ig+/Area Dapi+
E
BM Only
BM (WT) + T (WT)
BM (WT) + T (EZH2 KO)
BM (EZH2 KO Only)
BM (EZH2 KO) + T (WT)
Trichrome
F
BM Only
BM (WT) + T (WT)
BM (WT) + T (EZH2 KO)
BM (EZH2 KO Only)
BM (EZH2 KO) + T (WT)
Ig Deposition

Figure 4:

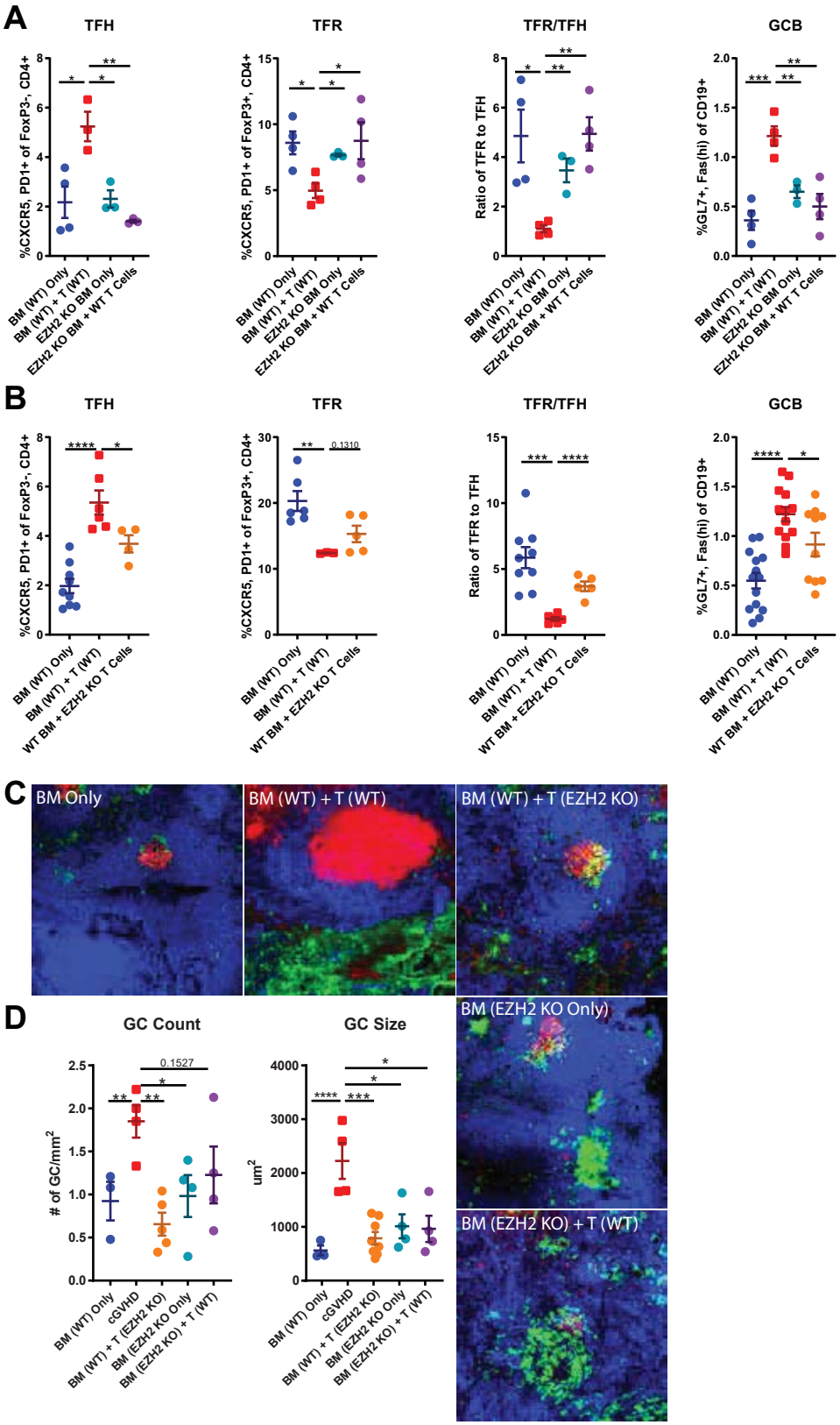
A
TFH
TFR
TFR/TFH
GCB
%CXCR5, PD1+ of FoxP3-, CD4+
%CXCR5, PD1+ of FoxP3+, CD4+
Ratio of TFR to TFH
%GL7+, Fas(hi) of CD19+
BM (WT) Only
BM (WT) + T (WT)
EZH2 KO BM Only
EZH2 KO BM + WT T Cells
B
TFH
TFR
TFR/TFH
GCB
%CXCR5, PD1+ of FoxP3-, CD4+
%CXCR5, PD1+ of FoxP3+, CD4+
Ratio of TFR to TFH
%GL7+, Fas(hi) of CD19+
0.1310
BM (WT) Only
BM (WT) + T (WT)
WT BM + EZH2 KO T Cells
C
BM Only
BM (WT) + T (WT)
BM (WT) + T (EZH2 KO)
BM (EZH2 KO Only)
BM (EZH2 KO) + T (WT)
D
GC Count
GC Size
# of GC/mm2
um2
0.1527
BM (WT) Only
cGVHD
BM (WT) + T (EZH2 KO)
BM (EZH2 KO Only)
BM (EZH2 KO) + T (WT)

Figure 5:

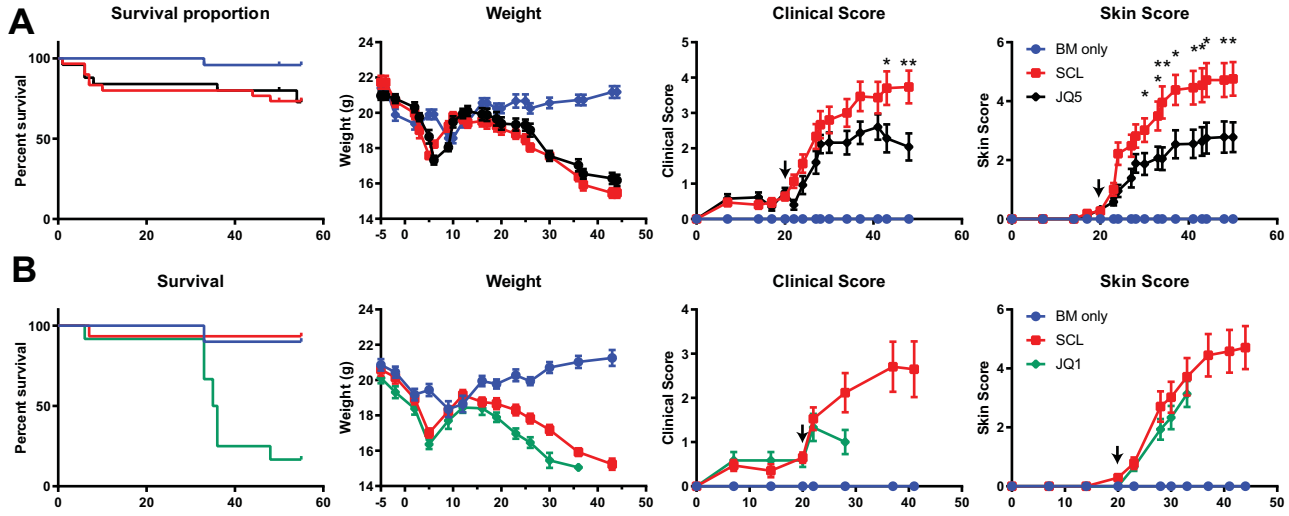
A
Survival proportion
Percent survival
Weight
Weight (g)
Clinical Score
Skin Score
BM only
SCL
JQ5
B
Survival
Percent survival
Weight
Weight (g)
Clinical Score
Skin Score
BM only
SCL
JQ1


C
BM Only
SCL
JQ5 Treated
JQ1 Treated

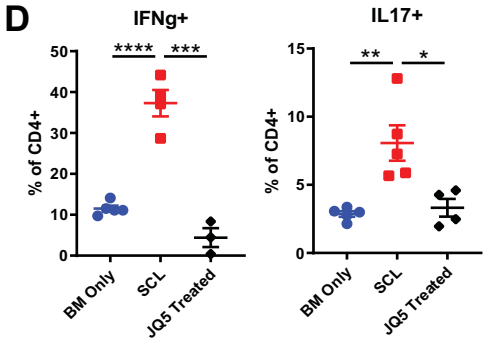
D
IFNg+
% of CD4+
****
***
BM Only
SCL
JQ5 Treated
IL17+
% of CD4+
**
*
BM Only
SCL
JQ5 Treated

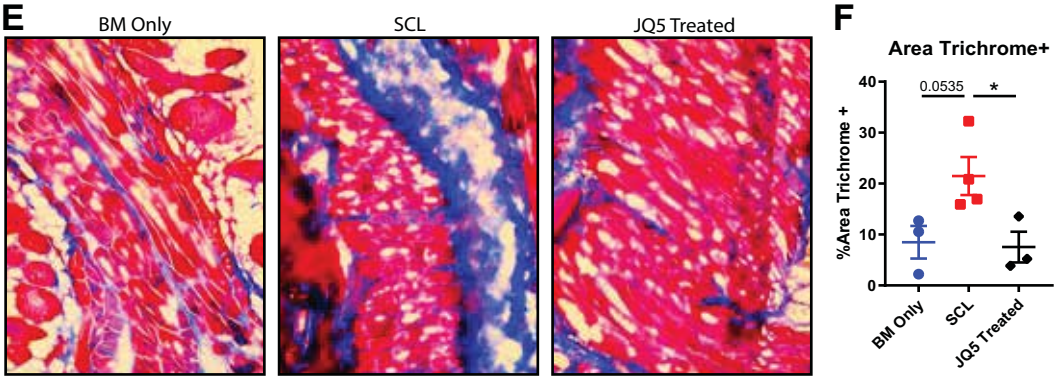
E
BM Only
SCL
JQ5 Treated

F
Area Trichrome+
%Area Trichrome +
0.0535
*
BM Only
SCL
JQ5 Treated

Figure 6:

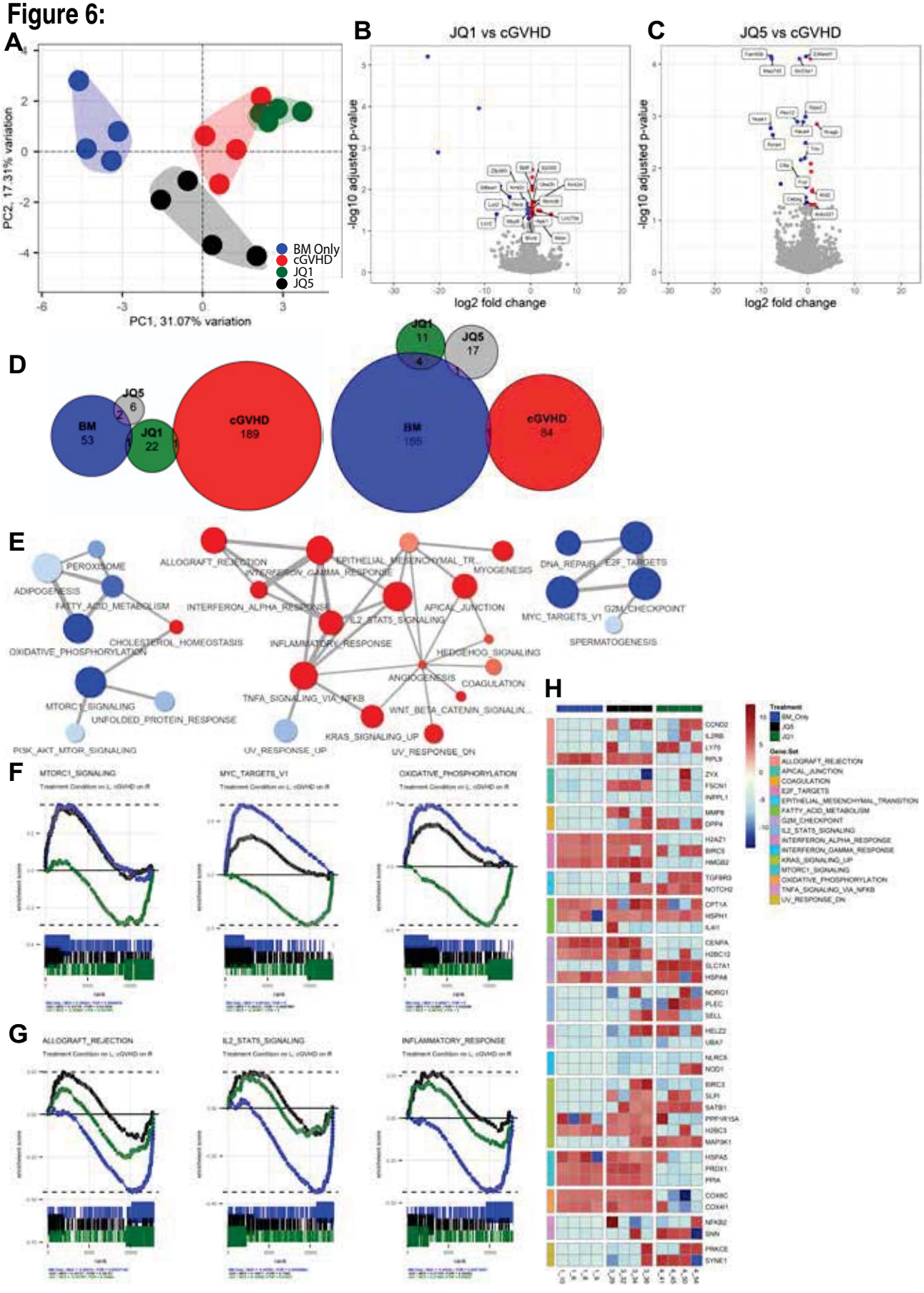
A
PC2, 17.31% variation
PC1, 31.07% variation
BM Only
cGVHD
JQ1
JQ5
B
JQ1 vs cGVHD
-log10 adjusted p-value
log2 fold change
C
JQ5 vs cGVHD
-log10 adjusted p-value
log2 fold change
D
JQ5
6
BM
53
JQ1
22
cGVHD
189
JQ1
11
JQ5
17
BM
155
cGVHD
84
E
PEROXISOME
ADIPOGENESIS
FATTY_ACID_METABOLISM
CHOLESTEROL_HOMEOSTASIS
OXIDATIVE_PHOSPHORYLATION
MTORC1_SIGNALING
UNFOLDED_PROTEIN_RESPONSE
PI3K_AKT_MTOR_SIGNALING
ALLOGRAFT_REJECTION
INTERFERON_GAMMA_RESPONSE
EPITHELIAL_MESENCHYMAL_TR...
MYOGENESIS
INTERFERON_ALPHA_RESPONSE
APICAL_JUNCTION
IL2_STAT5_SIGNALING
INFLAMMATORY_RESPONSE
HEDGEHOG_SIGNALING
ANGIOGENESIS
COAGULATION
TNFA_SIGNALING_VIA_NFKB
WNT_BETA_CATENIN_SIGNALIN...
KRAS_SIGNALING_UP
UV_RESPONSE_UP
UV_RESPONSE_DN
DNA_REPAIR
E2F_TARGETS
MYC_TARGETS_V1
G2M_CHECKPOINT
SPERMATOGENESIS
F
MTORC1_SIGNALING
MYC_TARGETS_V1
OXIDATIVE_PHOSPHORYLATION
G
ALLOGRAFT_REJECTION
IL2_STAT5_SIGNALING
INFLAMMATORY_RESPONSE
H
Treatment
BM_Only
JQ5
JQ1
Gene.Set
ALLOGRAFT_REJECTION
APICAL_JUNCTION
COAGULATION
E2F_TARGETS
EPITHELIAL_MESENCHYMAL_TRANSITION
FATTY_ACID_METABOLISM
G2M_CHECKPOINT
IL2_STAT5_SIGNALING
INTERFERON_ALPHA_RESPONSE
INTERFERON_GAMMA_RESPONSE
KRAS_SIGNALING_UP
MTORC1_SIGNALING
OXIDATIVE_PHOSPHORYLATION
TNFA_SIGNALING_VIA_NFKB
UV_RESPONSE_DN